



Published as: *Science*. 2013 November 29; 342(6162): 1098–1100.

## Non-enzymatic template-directed RNA synthesis inside model protocells

Katarzyna Adamala<sup>1,2</sup> and Jack W. Szostak<sup>1,\*</sup>

<sup>1</sup>Howard Hughes Medical Institute, Department of Molecular Biology, and Center for Computational and Integrative Biology, Massachusetts General Hospital, Boston, MA 02114, USA

<sup>2</sup>Dipartimento di Biologia, Università degli Studi di Roma Tre, Rome, Italy

### Abstract

Efforts to recreate a prebiotically plausible protocell, in which RNA replication occurs within a fatty acid vesicle, have been stalled by the destabilizing effect of  $Mg^{2+}$  on fatty acid membranes. Here, we report that the presence of citrate protects fatty acid membranes from the disruptive effects of high  $Mg^{2+}$  ion concentrations while allowing RNA copying to proceed, while also protecting single-stranded RNA from  $Mg^{2+}$ -catalyzed degradation. This combination of properties has allowed us to demonstrate the chemical copying of RNA templates inside fatty acid vesicles, which in turn allows for an increase in copying efficiency by bathing the vesicles in a continuously refreshed solution of activated nucleotides.

The RNA world hypothesis suggests that the primordial catalysts were ribozymes (1, 2), while biophysical considerations suggest that the primordial replicating compartments were membranous vesicles composed of fatty acids and related amphiphiles (3, 4). However, the conditions required for RNA replication chemistry and fatty acid vesicle integrity have appeared to be fundamentally incompatible (5) (Fig S1). Both ribozyme catalyzed and non-enzymatic RNA copying reactions require high (50–200 mM) concentrations of  $Mg^{2+}$  (or other divalent) ions (6), but  $Mg^{2+}$  at such concentrations destroys vesicles by causing fatty acid precipitation.

We developed a screen for small molecules that protect oleate fatty acid vesicles from disruption by  $Mg^{2+}$ . We used two assays to monitor the leakage of either a small charged molecule (calcein) or a larger oligonucleotide, allowing us to distinguish between increased

\*Correspondence to: Howard Hughes Medical Institute, Department of Molecular Biology, and Center for Computational and Integrative Biology, 7215 Simches Research Center, Massachusetts General Hospital, 185 Cambridge Street, Boston, MA 02114, Tel: 617-726-5981; Fax: 617-726-6893, szostak@molbio.mgh.harvard.edu.

Raw data are presented in the supplementary materials. The instructions for assembling the Liposome Dialyzer are available at <http://molbio.mgh.harvard.edu/szostakweb/>

List of supplementary content  
Materials and Methods  
Supplementary Text  
Figs. S1 to S21  
Tables S1 to S3  
Liposome Dialyzer instructions

membrane permeability (faster calcein release with oligonucleotide retention) and generalized membrane disruption (rapid release of both calcein and the oligonucleotide) (Fig. S2, S3 and S4). We identified several chelators, including citrate, isocitrate, oxalate, NTA and EDTA, that protect oleate vesicles in the presence of at least 10 mM  $Mg^{2+}$  (Fig. S5 and S6). In the presence of chelated  $Mg^{2+}$ , oleate vesicles remained intact but exhibited a modest increase in the permeability of a small polar molecule (Fig. 1 and S7) and an even smaller increase in the leakage of an oligonucleotide. In terms of vesicle stabilization, citrate was one of the most effective chelators of  $Mg^{2+}$ .

We also examined the stability of model protocell membranes made of myristoleic acid: glycerol monomyristoleate 2:1 and from the more prebiotically reasonable decanoic acid: decanol: glycerol monodecanoate 4:1:1. Citrate-chelated  $Mg^{2+}$  caused only a small amount of leakage from these vesicles, and the stabilizing effect of citrate was seen for both calcein and oligonucleotides (Fig. 1 and S8–S13).

We then asked if these chelators were compatible with the  $Mg^{2+}$  catalysis of non-enzymatic template-directed RNA primer extension. We measured the rate at which an RNA primer was elongated when annealed to an oligonucleotide with a templating region of C nucleotides, in the presence of excess activated G monomer, guanosine 5'-phosphor(2-methyl)imidazolide (2MeImpG) (Fig. 2). We examined citric acid, EDTA, NTA and a weakly stabilizing chelator (isocitric acid). In the presence of 50 mM unchelated  $Mg^{2+}$ , the primer-extension reaction proceeded at a rate of  $1.4 \text{ h}^{-1}$ , compared to  $0.03 \text{ h}^{-1}$  in the absence of  $Mg^{2+}$  ions. The addition of 4 equivalents of EDTA or NTA resulted in complete abolition of  $Mg^{2+}$  catalysis (Fig. 2 and S14, S15), indicating that the  $Mg^{2+}$  in these samples is chelated in a fashion incompatible with promoting primer extension. In contrast, four equivalents of citrate only decreased the rate of primer extension to  $0.67 \text{ h}^{-1}$ . For comparison, isocitric acid does not fully protect vesicles (Fig. S16 and S17), but also does not affect the primer extension reaction.

To see if citrate would allow non-enzymatic RNA copying to proceed within fatty acid vesicles, we encapsulated an RNA primer-template complex inside oleate vesicles, added  $Mg^{2+}$  and citrate, and removed unencapsulated RNA by size exclusion chromatography. We then added the activated G monomer 2MeImpG, heated the sample briefly to allow for rapid monomer permeation (7), and then incubated at room temperature for times up to 24 h to allow the monomer to take part in template-copying chemistry inside the vesicles. Analysis of the reaction products showed that after a 24 h incubation most of the primer had been extended by the addition of six G residues, with a smaller fraction extended to full length by the addition of a seventh G residue (Fig. 3). In parallel experiments with vesicles composed of mixtures of shorter-chain lipids, the brief heating step was not necessary, due to the higher permeability of such membranes to nucleotide monomers. It is noteworthy that RNA primer extension occurred efficiently inside vesicles made of decanoic acid: decanol: glycerol monodecanoate 4:1:1 (Fig. 3), since short chain, saturated amphiphilic compounds are more prebiotically plausible than longer chain, unsaturated fatty acids such as oleate or myristoleate. When we encapsulated the RNA primer-template complex inside POPC vesicles, no primer extension was observed, due to the impermeability of phospholipid vesicles to the 2MeImpG monomer (even with a heat pulse) (Fig. S18).

The efficiency of non-enzymatic RNA replication can be greatly enhanced by the periodic addition of fresh portions of activated monomer to a primer-extension reaction occurring on templates immobilized by covalent linkage to beads (8). We sought to reproduce this effect by mimicking the flow of an external solution of fresh monomers over vesicles, by periodic dialysis of model protocells against a solution of fresh activated monomers (See Supporting Materials for description of the Liposome Reactor Dialyzer). The control primer-extension reaction in solution shows that the yield of full length primer-extension product from copying a GCCG template is very low, even if fresh monomers are added to the reaction periodically (Figure 3E). In contrast, after repeated exchanges of external solution by dialysis, the proportion of full length product was much greater (Figure 3E).

The high thermal stability of the RNA duplex is a major problem for prebiotic RNA replication (5). Since  $Mg^{2+}$  greatly increases the  $T_m$  of RNA duplexes, we asked whether the chelating properties of citrate would prevent the increase in the melting temperature of RNA duplexes caused by the presence of free  $Mg^{2+}$  ions. We observed a small but reproducible decrease in  $T_m$  in the presence of citrate when compared to samples containing unchelated  $Mg^{2+}$  (Table S1, Figures S19 and S20). For example, in presence of 50 mM  $Mg^{2+}$  with 4 equivalents of citrate, the  $T_m$  of the RNA duplex was 71°C, while in the control sample without citrate the  $T_m$  was 75°C.

Citrate also stabilizes RNA by preventing the  $Mg^{2+}$  catalysis of RNA degradation. Incubating a 13-mer oligodeoxynucleotide with one *ribo* linkage at 75° C, with and without  $Mg^{2+}$  and citrate, results in significant strand cleavage at the site of the single *ribo* linkage. Four equivalents of citrate, relative to  $Mg^{2+}$ , abolished the  $Mg^{2+}$ -catalyzed degradation (Fig. 4). The  $k_{obs}$  for cleavage at the *ribo* linkage, at 75 °C in the presence of 50 mM  $Mg^{2+}$  was 0.074 hr<sup>-1</sup>, while in the presence of a 4-fold excess of citrate, the rate decreased to 0.004 hr<sup>-1</sup>.

The chelation of  $Mg^{2+}$  by citrate exhibits two protective effects in the context of model protocells: protocell membranes based on fatty acids are protected from the disruption caused by the precipitation of fatty acids as  $Mg^{2+}$  salts, and single-stranded RNA oligonucleotides are protected from  $Mg^{2+}$ -catalyzed degradation. Based on the known affinity of citrate for  $Mg^{2+}$  (9, 10), it is clear that the RNA synthesis observed in the presence of  $Mg^{2+}$  and citrate cannot be due to residual free  $Mg^{2+}$  (less than 1 mM), and must be due to catalysis by the  $Mg^{2+}$ -citrate complex. The crystal structure of  $Mg^{2+}$ -citrate (11) shows that the  $Mg^{2+}$  ion is coordinated by the hydroxyl and two carboxylates of citrate, such that three of the six coordination sites of octahedral  $Mg^{2+}$  are occupied by citrate, while the remaining three are free to coordinate with water or other ligands. The clear implication is that coordination of  $Mg^{2+}$  by at most three sites is sufficient for catalysis of template-directed RNA synthesis, but not for catalysis of RNA degradation or for the precipitation of fatty acids. In the absence of a prebiotic citrate synthesis pathway (but see ref. 12 for a recent advance), it is of interest to consider prebiotically plausible alternatives to citrate that could potentially confer similar effects, such as short acidic peptides. We note that just such a peptide constitutes the heart of cellular RNA polymerases, where it binds and presents the catalytic  $Mg^{2+}$  ion in the active site of the enzyme.

## Supplementary Material

Refer to Web version on PubMed Central for supplementary material.

## Acknowledgments

We thank Aaron Engelhart, Christian Hentrich, Aaron Larsen, Neha Kamat and Anders Björkbo for discussions and help with manuscript preparation and Ariella Gifford for help with vesicle leakage experiments.

This work was supported in part by NASA Exobiology grant NNX07AJ09G. J.W.S. is an Investigator of the Howard Hughes Medical Institute.

## References and Notes

1. Gilbert W. Origin of life: The RNA world. *Nature*. 1986; 319:618.
2. Joyce GF. RNA evolution and the origins of life. *Nature*. 1989; 338:217. [PubMed: 2466202]
3. Gebicki JM, Hicks M. Ufasomes are stable particles surrounded by unsaturated fatty acid membranes. *Nature*. 1973; 243:232. [PubMed: 4706295]
4. Deamer DW, Dworkin JP. Chemistry and physics of primitive membranes. *Top Curr Chem*. 2005; 1
5. Szostak JW. The eightfold path to non-enzymatic RNA replication. *J Sys Chem*. 2012; 3
6. Bowman JC, Lenz TK, Hud NV, Williams LD. Cations in charge: magnesium ions in RNA folding and catalysis. *Curr Opin Struct Bio*. 2012; 22:262. [PubMed: 22595008]
7. Mansy SS, Szostak JW. Thermostability of model protocell membranes. *Proc Nat Acad Sci USA*. 2008; 105:13351. [PubMed: 18768808]
8. Deck C, Jauker M, Richert C. Efficient enzyme-free copying of all four nucleobases templated by immobilized RNA. *Nat Chem*. 2011; 3:603. [PubMed: 21778979]
9. Covington AK, Danish EY. Measurement of Magnesium Stability Constants of Biologically Relevant Ligands by Simultaneous Use of pH and Ion-Selective Electrodes. *J Solution Chem*. 2009; 38:1449–1462.
10. Walser M. Ion Association V. Dissociation Constants For Complexes of Citrate With Sodium, Potassium, Calcium, And Magnesium Ions. *J Phys Chem*. 1961; 65:159–161.
11. Johnson CK. X-Ray Crystal Analysis of the Substrates of Aconitase. V. Magnesium Citrate Decahydrate. *Acta Crystallogr*. 1965; 18:1004. [PubMed: 14323450]
12. Butch C, et al. Production of Tartrates by Cyanide-Mediated Dimerization of Glyoxylate: A Potential Abiotic Pathway to the Citric Acid Cycle. *J Am Chem Soc*. 2013
13. Joyce GF, Inoue T, Orgel LE. Non-enzymatic template-directed synthesis on RNA random copolymers. Poly(C, U) templates. *J Mol Biol*. 1984; 176:279. [PubMed: 6205154]
14. Zhu TF, Adamala K, Zhang N, Szostak JW. Photochemically driven redox chemistry induces protocell membrane pearling and division. *Proc Nat Acad Sci USA*. 2012; 109:9828. [PubMed: 22665773]
15. Zhu TF, Szostak JW. Coupled growth and division of model protocell membranes. *J Am Chem Soc*. 2009; 131:5705. [PubMed: 19323552]

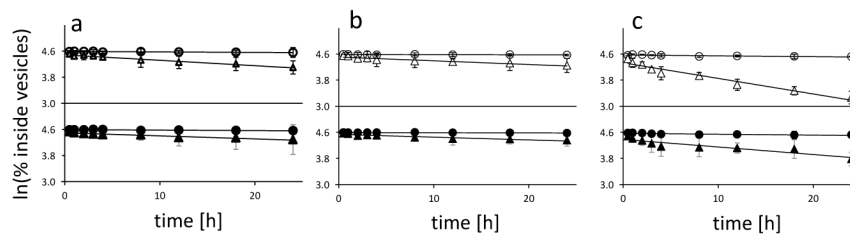


**Figure 1. Citrate stabilizes fatty acid vesicles in the presence of  $Mg^{2+}$  ions**

Leakage of a small charged molecule (calcein, open symbols) and a larger 9-mer oligodeoxynucleotide (filled symbols) from fatty acid vesicles. A: oleate vesicles; B: myristoleate: glycerol monomyristoleate 2:1 vesicles; C: decanoate: decanol: glycerol monodecanoate 4:1:1 vesicles. Circles: no  $MgCl_2$ , no citrate; triangles: 50 mM  $MgCl_2$ , 200 mM  $Na^+$ -citrate.

The assay used to obtain this data is described in Figure. Lines are linear fits,  $R^2 = 0.97$ . All experiments were repeated twice, error bars are mean  $\pm 2SE$ .

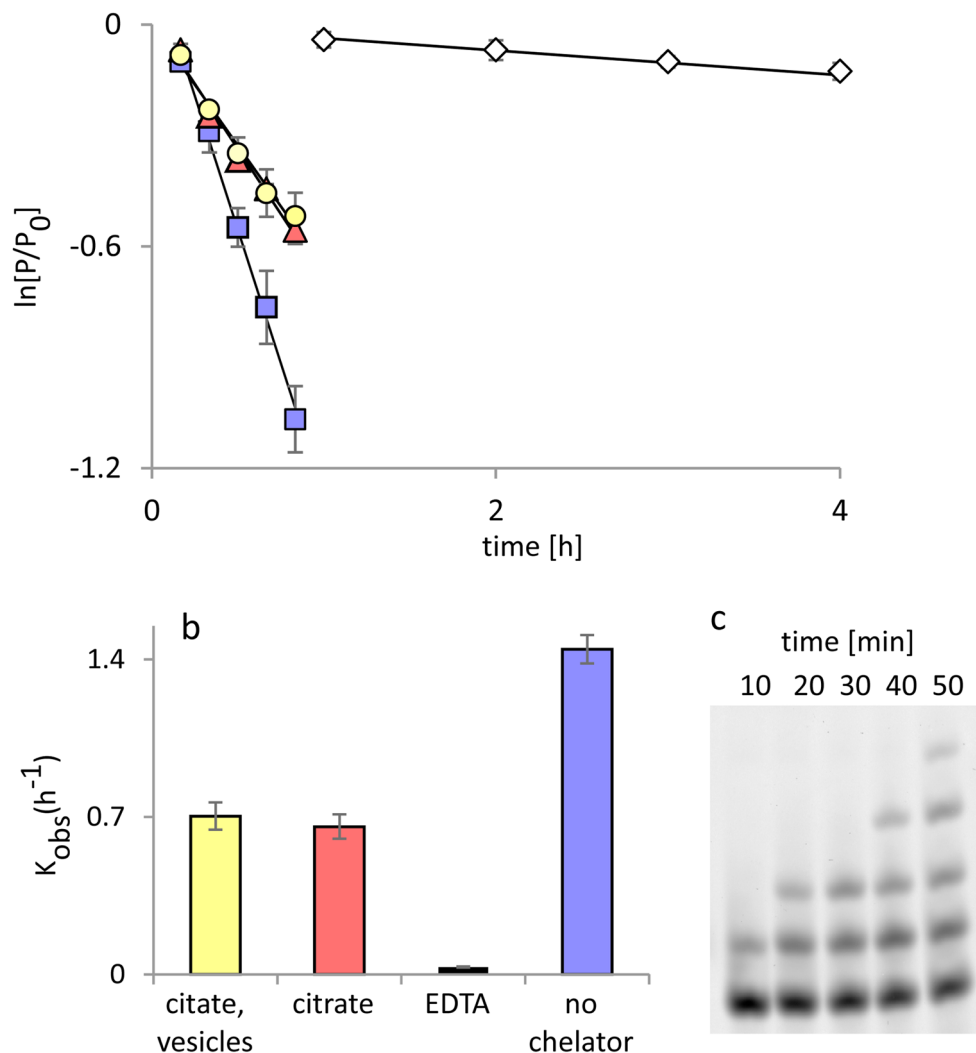


**Figure 2. The rate of RNA template-directed primer extension in the presence or absence of Mg<sup>2+</sup> chelators and fatty acid vesicles**

**A:** Time courses of primer extension on a templating region of four C residues, expressed as fraction of un-extended primer remaining vs. time. Squares: no chelators; triangles: 200 mM Na<sup>+</sup>-citrate; circles: 200 mM Na<sup>+</sup>-citrate and 100 mM oleate vesicles; diamonds: 200 mM EDTA. Lines are linear fits,  $R^2 = 0.97$ ; the slope is  $k_{obs}$  (h<sup>-1</sup>).

**B:** Rates of primer extension under the indicated conditions; each kinetic experiment was performed in duplicate and rates are determined as average of the three separate runs. Error bars indicate SEM,  $n=3$ .

**C:** Typical PAGE analysis of a template-directed primer extension experiment. Primer extension was carried out in the presence of 200 mM Na<sup>+</sup>-citrate.

For the gel analysis of the reactions used to obtain this data, see Supporting Information Figure S15.

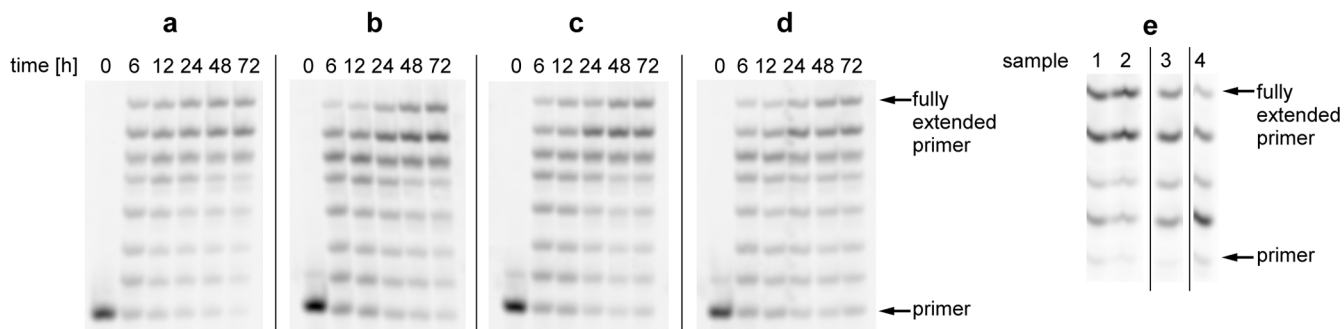


**Figure 3. RNA template copying inside model protocell vesicles**

A to D: Primer extension on a templating region of seven C residues. **A:** control reaction in solution; **B:** inside oleate vesicles, **C:** inside myristoleate: glycerol monomyristoleate 2:1 vesicles; **D:** inside decanoate: decanol: glycerol monodecanoate 4:1:1 vesicles. **E:** Extension of labeled RNA primer annealed to a mixed base template, templating region sequence GCCG.

Sample 1: reaction inside myristoleate: glycerol monomyristoleate 2:1 vesicles, sample 2: reaction inside decanoate: decanol: glycerol monodecanoate 4:1:1 vesicles, both sample 1 and 2 reactions performed inside liposome dialyzer (see Supplementary Materials for the description of the liposome dialyzer) with a total of 13 buffer exchanges. Sample 3: control reaction in solution with daily addition of fresh portion of activated monomers, without removing the hydrolyzed monomers. Sample 4: control reaction in solution, without addition of fresh monomer.

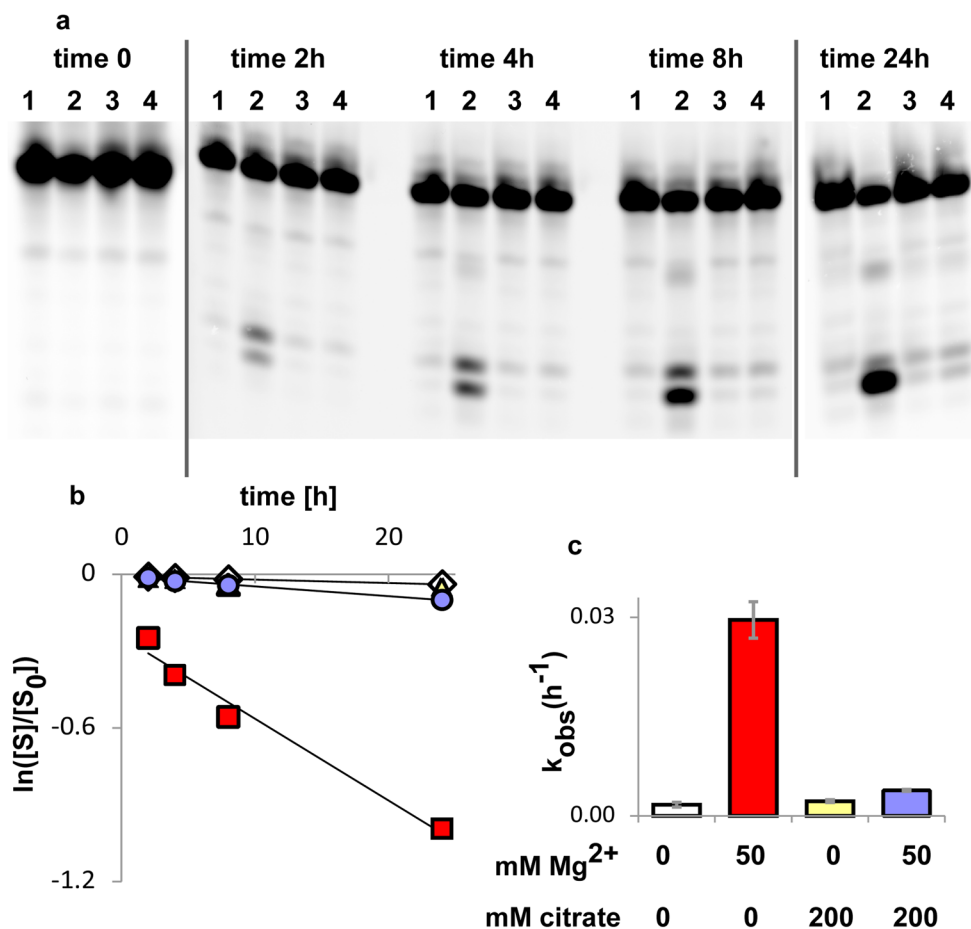


**Figure 4. Citrate protects RNA from Mg<sup>2+</sup>-catalyzed degradation**

**A:** PAGE analysis of cleavage of a DNA oligonucleotide at the site of a single internal ribonucleotide, at indicated time points; lanes 1: no Mg<sup>2+</sup>, no citrate; lanes 2: 50 mM Mg<sup>2+</sup>, no citrate; lanes 3: no Mg<sup>2+</sup>, 200 mM citrate; lanes 4: 50 mM Mg<sup>2+</sup>, 200 mM citrate.

**B:** Quantitation of strand cleavage, expressed as fraction of intact substrate over total substrate vs. time: diamonds: no Mg<sup>2+</sup>, no citrate; triangles: no Mg<sup>2+</sup>, 200 mM citrate; circles: 50 mM Mg<sup>2+</sup>, 200 mM citrate; squares 50 mM Mg<sup>2+</sup>, no citrate. Lines are linear fits, R<sup>2</sup> = 0.97.

**C:** Rates of strand cleavage at the *ribo* linkage with and without Mg<sup>2+</sup> and citrate. Error bars indicate SEM, n=3.